Controllable Preparation of Submicrometer Single-Crystal C60 Rods and Tubes Trough Concentration Depletion at the Surfaces of Seeds

ARTICLE *in* THE JOURNAL OF PHYSICAL CHEMISTRY C · JUNE 2007

Impact Factor: 4.77 · DOI: 10.1021/jp071912r

8 AUTHORS, INCLUDING:

Hengxing Ji
University of Science and Technology of China
41 PUBLICATIONS **1,832** CITATIONS
SEE PROFILE

Jin-Song Hu
Chinese Academy of Sciences
75 PUBLICATIONS **6,613** CITATIONS
SEE PROFILE

Wei-Guo Song
Chinese Academy of Sciences
110 PUBLICATIONS **4,493** CITATIONS
SEE PROFILE

Chun-Ru Wang
Chinese Academy of Sciences
66 PUBLICATIONS **2,116** CITATIONS
SEE PROFILE

Controllable Preparation of Submicrometer Single-Crystal C_{60} Rods and Tubes Trough Concentration Depletion at the Surfaces of Seeds

Heng-Xing Ji,[†,‡] Jin-Song Hu,[†] Qing-Xin Tang,[†,‡] Wei-Guo Song,[†] Chun-Ru Wang,[†] Wen-Ping Hu,[†] Li-Jun Wan,*[,†] and Shuit-Tong Lee*[,§]

Beijing National Laboratory for Molecular Sciences (BNLMS), Institute of Chemistry, Chinese Academy of Sciences (CAS), Beijing 100080, China, Graduate School of CAS, Beijing, China, and Center of Super-Diamond and Advanced Films (COSDAF) and Department of Physics and Chemistry, City University of Hong Kong, Hong Kong SAR, China

Received: March 9, 2007; In Final Form: May 8, 2007

Single-crystal submicrometer rods and tubes of C_{60} with highly uniform size and shape were produced from a solvent-induced and surfactant assisted self-assembly technique. The length and length-to-width ratio of both rods and tubes were tunable by controlling the concentration of C_{60} in the stock solution. The transformation from rod to tube was achieved by simply varying the volume ratio of two solvents. Fourier-transform infrared and Raman spectroscopy, X-ray diffraction and high-resolution transmission electron microscopy revealed the detailed structures of the rods and tubes. We proposed a concentration profile based growth model to describe the self-assembly process of C_{60} subunits. This study may contribute to better understanding of chemistry of fullerenes in solutions and extend the surfactant-assisted self-organization of inorganic system to fullerene system.

Introduction

C_{60} and its derivates, as a new type of carbon materials with unique properties,[1−3] are of tremendous interest in diverse areas.[4−8] For the applications of C_{60} material, one remaining challenge is to produce it with predesigned and controllable structures within the submicrometer or nanometer scale. One-dimensional (1D)[9−12] C_{60} submicrometer materials, including rods or tubes with controllable sizes and morphologies, are desirable both for a fundamental and a practical point of view. Recently, C_{60} nanotubes were fabricated using alumina membrane as template.[13,14] We also developed an alumina membrane based electrochemical method[15−17] to fabricate well-defined C_{60} nanowire and nanotube arrays with controlled size and orientations. Another work of which we aware is that by Minato and Miyazawa et al. who have developed a liquid−liquid interfacial precipitation (LLIP) method to produce C_{60} submicrometer whiskers and tubes.[18−22] They have systematically studied the crystal structure of these C_{60} whiskers and have developed a series of method based on LLIP method to achieve C_{60} 1D structures. Liu et al. have developed a simple method to prepare C_{60} nanorods by dropwise addition of C_{60} solution onto a certain substrate at various temperatures.[23] Most recently, synthesis of C_{60} single-crystal rod with face-centered cubic structure is reported.[24] However, the detailed mechanism of C_{60}material formation, as well as controlled fabrication of single-crystal C_{60} 1D structure, rods and tubes, with desirable morphologies and designed size, is still elusive.

Herein, we report a reliable and facile solvent-induced self-assembly method[25] to produce C_{60} single-crystal 1D submicrometer rods and tubes with controllable size and morphologies. The length aspect ratio of the 1D materials are readily tuned by varying the concentration of C_{60} in *m*-xylene, and their morphologies can be chosen from rod to tube by using different *m*-xylene/isopropanol volume ratio. We propose a C_{60} concentration profile controlled growth mechanism to explain the self-assembly process of C_{60} 1D submicrometer structure. The present work shows that it is possible to produce C_{60} rods or tubes simply by tuning the reaction conditions. It may also contribute to better understanding the chemistry of fullerenes in solutions.

Results and Discussion

When 6 mL of C_{60}/*m*-xylene stock solution with different C_{60} concentrations (ranging from 0.75 mg/mL to 1.5 mg/mL) was injected into vigorously stirred 6 mL of cetyltrimethylammonium bromide (CTAB, 5 mM)/isopropanol solution at room temperature, the colorless solution turned to clear mauve immediately. Within 15 s, the solution became turbid mauve and then turbid lemon-yellow. After 10 min of continuous stirring, a C_{60} submicrometer rod was formed. The solid samples were recovered by centrifugation and washing with ethanol to remove surfactant residua. Figures 1a−d depicts the Scanning Electronic Microscopy (SEM) images of a series of C_{60} submicrometer rods, indicating that the length/width ratio of the rods could be readily tuned by varying the concentration of C_{60} in *m*-xylene. For example, samples 1, 2, and 3 were prepared under identical conditions except for the different C_{60} concentration in *m*-xylene at 0.75, 1.0, and 1.2 mg/mL, respectively, and the average length of the corresponding rods obtained was 25, 10, and 3 μm (Figure 1a,b,c), respectively. High magnification SEM image of sample 3 (Figure 1d) reveals that the rods have a regular hexagonal cross section with a 6-fold symmetry along the rod axis. The average width, *w*, between the opposite arrises of the rods was about 400 nm. Notably, the SEM images show that increasing C_{60} concentration in *m*-xylene caused little

* Corresponding author. E-mail: wanlijun@iccas.ac.cn, apannale@cityu.edu.hk.
† Institute of Chemistry, CAS.
‡ Graduate School of CAS.
§ City University of Hong Kong.

10.1021/jp071912r CCC: $37.00
Published on Web 06/22/2007

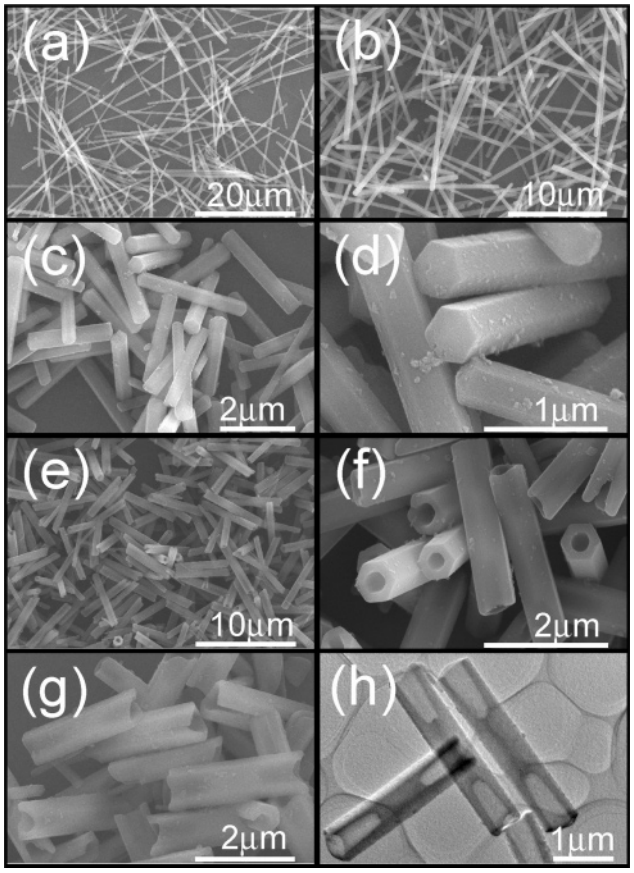

Figure 1. Electronic microscopy images of submicrometer rods (a−d) and tubes (e−g) of C_{60}. Typical SEM images of sample 1 (a) and sample 2 (b). Low (c) and high (d) magnification SEM images of sample 3. SEM images of sample 4 (e), sample 5 (f), and sample 6 (g) show a tubular feature of these samples. TEM image of submicrometer tubes (h).

change in the width of the hexagonal rods; while the rod length was substantially affected.

Furthermore, as shown in the SEM images (Figure 1e−g), by reducing the *m*-xylene/isopropanol ratio, the C_{60} molecules self-assembled into a submicrometer tubes. Figures 1e and 1f show typical SEM images of sample 4 and 5 (the preparation process are detailed in Experimental Section), in which every 1D structure possessed a hexagonal cross section and a circular open end. The tubes in each sample had uniform length and nearly the same width (*w*) as well as the same open circle's diameter (*d*). The length of the tubes in sample 4 and 5 was about 5 μm and 3 μm, respectively. The transmission electronic cicroscopy (TEM) image in Figure 1h shows tubular features on both ends as well as the solid center. Moreover, the *d*/*w* ratio of the submicrometer hexagonal tube was also tunable by varying the *m*-xylene/isopropanol volume ratio. Sample 6 was prepared with the same condition as sample 5 except the *m*-xylene/isopropanol volume ratio was 1:3 instead of 1:2. SEM image of sample 6 (Figure 1g) reveals that the average open circle's diameter (*d*) was about 520 nm and the average width (*w*) between two opposite arrises was about 800 nm, whereas the *d* and *w* value of sample 5 (Figure 1f) was about 300 and 650 nm, respectively. The *d*/*w* ratio of sample 6 was 0.65, and that of sample 5 was 0.46. The detailed preparation conditions for all samples in this study are shown in Table 1.

To confirm the composition and the crystalline nature of the 1D submicrometer materials, Fourier Transform Infrared (FTIR), Raman spectra, and X-ray diffraction (XRD) pattern of all samples were recorded. FTIR spectrum (Figure 2a) has four relatively strong and sharp absorption peaks at 1429.2, 1183.3, 576.7, and 526.5 cm^{-1}, which are the characteristic bands of pristine C_{60},[26,27] and two weak and broad peaks at 766.7 and 689.5 cm^{-1}, suggesting the presence of residual *m*-xylene solvent molecules trapped in the structure.[20,23] Previous studies showed that polymerization of C_{60} usually gave rise to new absorption bands and frequency shifts, due to the reduction of I_h symmetry of C_{60} molecule.[26,28] However, none of these spectral changes was observed from the IR spectrum, indicating that C_{60} 1D structure is consisted of unpolymerized pristine C_{60}. In addition, there is no other absorption peak in Figure 2a except that mentioned above, indicating that most surfactant was removed from C_{60} rods and tubes by ethanol wash. The Raman spectrum (Figure 2b) shows ten scattering peaks with varying intensities that are characteristic features of monomeric pristine C_{60} molecules.[26,29,30] All samples obtained in this study, both rods and tubes, show the same IR and Raman spectra. XRD pattern (Figure 2c) of C_{60} materials shows sharp and intensive peaks that are similar to that of the reported C_{60} bulk crystals[31] and the C_{60} submicro whiskers,[20] suggesting that these C_{60} submicro 1D materials in this study are crystals with a rhombohedral space group $P6_3$ and a unit cell dimensions of $a = b = 23.67$ Å, $c = 10.02$ Å, $\alpha = \beta = 90°$, and $\gamma = 120°$.[31]

High-resolution transmission electron microscopy (HRTEM) image and selected area electron diffraction (SAED) pattern of C_{60} rod are acquired (Figure 3) to investigate the details of the crystal structure. The black line along the center of the rod (Figure 3a) indicated that this C_{60} rod is lying with one arris on the HRTEM grid. Figure 3b,c show the representative SAED pattern and HRTEM image taken from the area circled in Figure 3a. Significantly, the same SAED pattern and the continuous lattice fringes in HRTEM image are obtained along the whole hexagonal rod, demonstrating the rod is indeed a single crystal. The discrete diffraction spots in Figure 3b are indexed according to the rhombohedral structure, in which the [001] direction was parallel to the longitudinal axis of the hexagonal rod, and the *d* $(10\bar{1}0)$ as well as *d*(0001) lattice spacing are 2.09 and 1.01 nm, respectively. From the HRTEM image in Figure 3c, the distance between two adjacent planes is 2.10 nm, very close to *d* $(10\bar{1}0)$, indicating that the side surface of the submicro hexagonal rod is $(10\bar{1}0)$ plane. This result is in good agreement with the SAED pattern. By the analysis of XRD and HRTEM,

TABLE 1: Shapes, Length, Width, and Inner Diameter of C_{60} 1D Structure Obtained at Different Preparation Conditions

sample number	volume ratio (isopropanol/ *m*-xylene)	C_{60} concentration (mg/mL)	shape	length (μm)	width (nm)	inner diameter (nm)
1	1:1	0.75	rod	25.0 ± 1.4	447 ± 13	
2	1:1	1.00	rod	10.0 ± 0.3	412 ± 11	
3	1:1	1.20	rod	3.0 ± 0.1	406 ± 15	
4	1:2	1.00	tube	5.0 ± 0.3	668 ± 28	301 ± 16
5	1:2	1.20	tube	3.0 ± 0.1	653 ± 27	316 ± 13
6	1:3	1.20	tube	3.0 ± 0.2	811 ± 50	520 ± 31

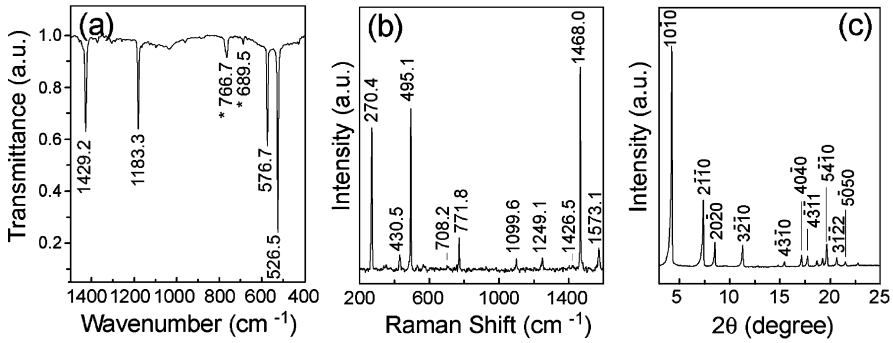

Figure 2. FTIR absorption spectrum (a) and Raman scattering spectrum (b) of C_{60} 1D structure. The asterisks in panel a indicate the solvent peaks. XRD pattern (c) of self-assembled C_{60} 1D submicrometer structure.

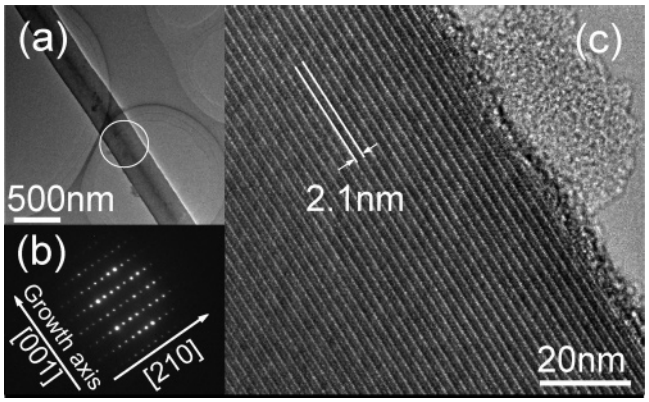

Figure 3. Low-magnification TEM image (a), selected area electron diffraction patterns (b) and high-resolution TEM image (c) of a C_{60} rod.

we conclude that the C_{60} 1D structures have a rhombohedral space group $P6_3$ and the longitudinal axis of them was parallel to the [001] direction.

On the basis of these experimental findings, a growth mechanism to describe the formation process of these samples is proposed in Figure 4. The growth process of C_{60} 1D submicro structure is controlled by the intrinsic properties of C_{60} crystal and C_{60} concentration profile on the surface of crystal seeds. Previous work[32−35] have reported that C_{60} and C_{70} colloids with narrow size distributions were immediately formed when the solution of fullerenes in a good solvent was fast injected into a poor solvent. Due to the highly anisotropic nature of these crystal seeds,[34] the growth direction was largely confined to the [001] direction, resulting in one-dimensional structures.[36] During the crystal growth after nucleation, the C_{60} molecules prefer the corners of the hexagonal cross section, as indicated by the black solid arrows in Figure 4, because the corner sites have a relatively higher free energy.[37] The secondarily preferable sites for C_{60} molecules are the edges of the hexagonal cross section, as indicated by the red dashed arrows in Figure 4. Finally is the central portion of the hexagonal cross section. When the volume ratio of *m*-xylene/isopropanol is 1:2, the solubility of C_{60} molecules in the mixed solvent is poor; and when a crystal seed is formed and starts to grow, it will suffer from C_{60} concentration depletion immediately after the nucleation.[36] C_{60} molecules are preferably attached to the preferred growing sites (corners and edges), but not the central portions of the growing faces of each seed, which results in the formation of hexagonal tubes with well-defined hollow interiors. When the *m*-xylene/isopropanol volume ratio is further decreased (such as 1:3), the concentration depletion effect becomes more severe, so that the *d*/*w* ratio of each tube will increase. Such nucleation-induced concentration depletion has also been observed in some inorganic colloidal systems.[36,38,39] Because the growth rate of both (0001) and (000$\bar{1}$) planes are the same, the final structure represents two hexagonal tubes sharing a solid center. Such morphology was also obtained in inorganic system by Xia et al.[36] On the other hand, when the volume ratio of *m*-xylene/isopropanol is increased to 1:1, the concentration of C_{60} in solution is high enough to absorb the concentration depletion effect in the central portion of the growing faces, leading to the formation of the rod like structure.

The growth kinetics of C_{60} rods and tubes formation are studied by collecting samples shortly after the solutions are mixed. Figures 5a−c show the SEM images of C_{60} rod at various stages. Two seconds after the initiation (Figure 5a), preliminary rod is formed with grooves at each side-face center of the rod, and these grooves become narrow, finally disappear while extending along the rod. At five seconds after initiation (Figure 5b), the grooves are narrower and the rods are longer. Finally, grooves are disappeared and full rods are formed (Figure 5c). Such morphology change can be explained by the mechanism we proposed. The grooves represent the C_{60} concentration profile around the rods. At the beginning, nucleation causes temporary concentration depletion around the crystal seeds. When the rods start growing, since the C_{60} concentration is low, C_{60} molecules deposit mainly at the preferable corner sites of the core seeds, and not the edge sites. Consequently, grooves are formed at the center of each side face. Such nucleation induced concentration depletion is limited to a small space around each seeds,[38,39] so when the rods are growing beyond the concentration depleted region, the C_{60} molecule concentration is high enough to deposit not only at the corner but also at the edge and central portion of the (0001) face, resulting in the narrowing and eventually disappearance of the grooves along the rod growth direction (Figure 5a). In addition, nucleation induced concentration depletion is temporary. After enough time, the mass transfer will offset the concentration depletion, and the C_{60} molecules can fill up the grooves (Figure 5b,c). These grooves are also observed at the early stage on the C_{60} tube surface (Shown in Supporting Information Figure S1).

According to this mechanism, we expect that when the volume ratio of *m*-xylene/isopropanol is further decreased, the concentration depletion effect will limit the growths at only the corner sites of every solid seed. As a result, a fence-like structure with six sticks standing upright on both (0001) and (000$\bar{1}$) planes of a solid core would occur. Sample 7 was prepared with the same condition as sample 5 except that the *m*-xylene/isopropanol volume ratio was further decreased to 1:5. Typical SEM images of sample 7 (Figure 5d−f) show indeed a fence-like structure with six parallel sticks stemming from a solid core.

Alargova et al.[34] reported that changing C_{60} concentration in a good solvent from about 0.75 to 1.5 mg/mL had little effect

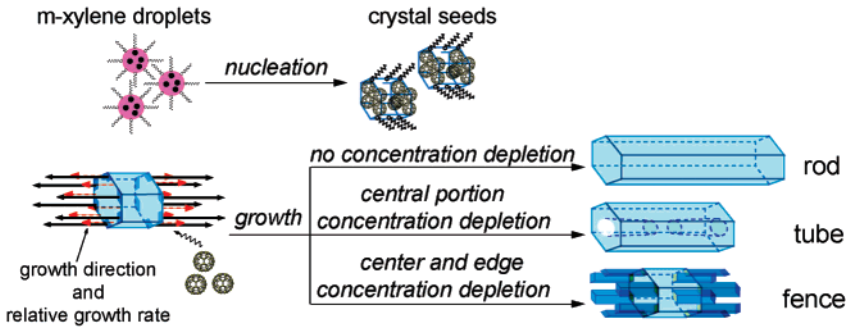

Figure 4. Schematic illustration of the formation process of C_{60} 1D submicrometer structures. The black solid arrows and red dashed arrows on the crystal seed represent different growth rates.

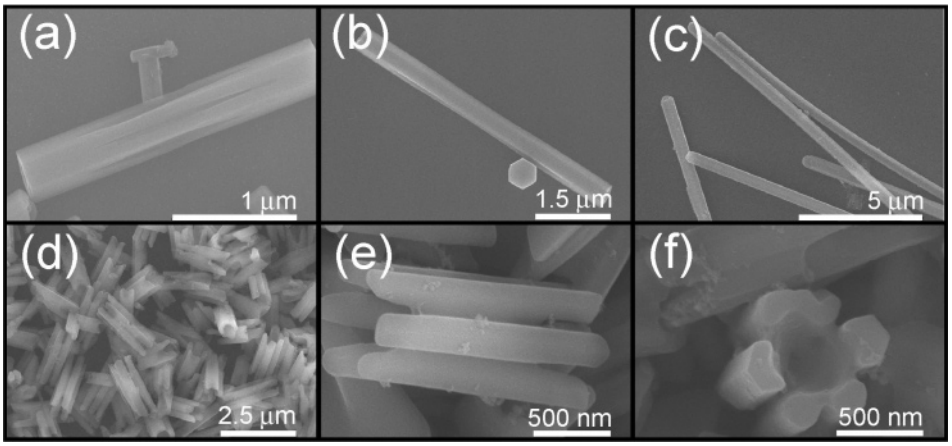

Figure 5. SEM images of morphology evolution of C_{60} rod (a−c) and fence-like structure (d−f) of C_{60}. C_{60} rod obtained at 2 s (a) and 5 s (b) after C_{60} solution injecting into isopropanol, and integrated C_{60} rod (c) obtained after 10 min. Low-magnification SEM image (d) of fence-like structure, and high-magnification SEM images of the side view (e) and top view (f) of the fence-like structure.

on the seed size, whereas reducing the volume ratio of a good solvent to a poor solvent resulted in increasing seed sizes. Therefore, all 1D structures produced from different C_{60} concentrations but with the same *m*-xylene/isopropanol volume ratio had nearly the same width. However, when the *m*-xylene/isopropanol volume ratio was decreased, the width of 1D structure increases. Some researchers have suggested that the rate of growth of a crystal face is a function of the degree of supersaturation at that face.[36,37] In this study, reducing C_{60} concentration in stock solution extends the duration of the color change stage, indicating a longer growth process of C_{60} 1D structures, and C_{60} molecules would have more time to transfer and deposit on (0001) face. As a result, the 1D structure with a larger length/width ratio is obtained.

The effect of CTAB on producing 1D C_{60} submicro structures is also investigated. Two samples are prepared with the same condition as sample 2 (shown in Figure 1b) except that CTAB concentration in isopropanol is 0 mM and 0.5 mM, respectively. The SEM images of these samples (Shown in Supporting Information Figures S2 and S3) show that C_{60} molecules could also form 1D structures without CTAB, but the structures have nonuniform sizes along with some small seeds. The small seeds disappear when CTAB concentration is increased to 0.5 mM, yet the 1D structure are still not as uniform as sample 2 in Figure 1b. We believe that CTAB molecules assist the crystallization process of C_{60} molecules. Similar influence of CTAB or other surfactants on crystal morphologies has been reported in earlier works.[40,41]

Conclusion

In summary, an effective and facile method is developed to controllable fabricate C_{60} 1D submicrometer structures with uniform size and tunable shape. The morphology of the structure can be readily tailored from hexagonal rod to hexagonal tube by changing the ratio of a good solvent to a poor solvent. The C_{60} 1D submicrometer structures are identified single crystals of C_{60} monomers with the rhombohedral space group $P6_3$. A model based on concentration profile controlled growth was proposed to describe the formation process of C_{60} 1D submicrometer structures. Future work will focus on the potential applications of these materials in miniature devices.

Experimental Section

C_{60} was synthesized by dc arc-discharge method and isolated by multiple-step high-performance liquid chromatography (Japan Analytical Industry Co., LTD) with Buckyprep and Buckyclutchar columns.

In a typical preparation procedure for single-crystal submicrometer rod, 6 mL of stock C_{60} and *m*-xylene (Beijing Chemical Reagent Corp., China) solution with various C_{60} concentrations was injected into 6 mL of continuously stirred isopropanol (Beijing Chemical Reagent Corp., China) solution of CTAB (Aldrich Chemical Co., USA) (5 mM) at room temperature. The mixture was stirred for 10 min. Solid sample was recovered by centrifugation and washing with ethanol (Beijing Chemical Reagent Corp., China) twice. Three samples with the concentration of C_{60} (C_{C60}) = 0.75, 1.0, and 1.2 mg/mL were prepared, and were named as sample 1, 2 and 3 respectively. For the preparation of submicrometer tubes (sample 4 and 5) in this study, 3 mL of stock C_{60} in *m*-xylene solution with the concentration of C_{60} (C_{C60}) = 1.0 and 1.2 mg/mL was injected into 6 mL isopropanol solution of CTAB (5 mM) under continuous stirring at room temperature. After 10 min of continuously stirring, the resulted suspension was centrifugal

separated from solution and washed with ethanol twice to remove the surfactant.

For electron microscopy observation, the ethanol suspension of synthesized product was deposited onto silicon wafer substrate and copper grid for SEM and TEM characterization, respectively. A Hitachi S-4300F scanning electron microscopy was used to investigate the morphology of the C_{60} 1D submicrometer structure. TEM images were collected from a TECNAI F30 operating at 300 kV. FTIR spectrum was obtained with KBr pellet on a Bruker Tensor 27 FT-IR spectrometer. Raman scattering spectrum was recorded on a Bruker RFS 100 Raman spectrometer with a laser of 1064.4 nm at a power density of 50 $mW \cdot mm^{-2}$. X-ray diffraction measurement was carried out with a Rigaku D/max-2500 using filtered Cu Kα radiation.

Acknowledgment. This work is partially supported by National Natural Science Foundation of China (Grant Nos. 20121301, 20520140277, 20603041, 20673121, and 20575070), the National Key Project on Basic Research (Grant No. 2006CB806100), and the Chinese Academy of Sciences.

Supporting Information Available: The SEM images of C_{60} tubes obtained at various stages, and the SEM images of C_{60} rods acquired without the assistant of CTAB are available. This material is available free of charge via the Internet at http://pubs.acs.org.

References and Notes

(1) Yamanaka, S.; Hotehama, K.; Kawaji, H. *Nature* **1998**, *392*, 580.
(2) Huang, H. J.; Gu, G.; Yang, S. H.; Fu, J. S.; Yu, P.; Wong, G. K. L.; Du, Y. W. *J. Phys. Chem. B* **1998**, *102*, 61.
(3) Huang, H. J.; Yang, S. H.; Zhang, X. X. *J. Phys. Chem. B* **2000**, *104*, 1473.
(4) Taylor, R.; Walton, D. R. M. *Nature* **1993**, *363*, 685.
(5) Dresselhaus, M. S.; Dresselhaus, G.; Eklund, P. C. *Science of Fullerenes and Carbon Nanotubes*; Academic Press: San Diego, 1996.
(6) Guan, L. H.; Suenaga, K.; Shi, Z. J.; Gu, Z. N.; Iijima, S. *Phys. Rev. Lett.* **2005**, *94*.
(7) Dennis, T. J. S.; Hulman, M.; Kuzmany, H.; Shinohara, H. *J. Phys. Chem. B* **2000**, *104*, 5411.
(8) Hu, X. Q.; Jiang, Z. P.; Jia, Z. S.; Huang, S. H.; Yang, X. B.; Li, Y. L.; Gan, L. B.; Zhang, S. W.; Zhu, D. B. *Chem. Eur. J.* **2007**, *13*, 1129.
(9) Xia, Y. N.; Yang, P. D.; Sun, Y. G.; Wu, Y. Y.; Mayers, B.; Gates, B.; Yin, Y. D.; Kim, F.; Yan, Y. Q. *Adv. Mater.* **2003**, *15*, 353.
(10) Cui, Y.; Wei, Q. Q.; Park, H. K.; Lieber, C. M. *Science* **2001**, *293*, 1289.
(11) Zhang, G. M.; Zhang, J.; Xie, G. Y.; Liu, Z. F.; Shao, H. B. *Small* **2006**, *2*, 1440.
(12) Zhang, X. J.; Zhang, X. H.; Shi, W. S.; Meng, X. M.; Lee, C. S.; Lee, S. T. *Angew. Chem., Int. Ed.* **2007**, *46*, 1525.
(13) Gan, H. Y.; Liu, H. B.; Li, Y. L.; Gan, L. B.; Jiang, L.; Jiu, T. G.; Wang, N.; He, X. R.; Zhu, D. B. *Carbon* **2005**, *43*, 205.
(14) Liu, H. B.; Li, Y. L.; Jiang, L.; Luo, H. Y.; Xiao, S. Q.; Fang, H. J.; Li, H. M.; Zhu, D. B.; Yu, D. P.; Xu, J.; Xiang, B. *J. Am. Chem. Soc.* **2002**, *124*, 13370.
(15) Guo, Y. G.; Wan, L. J.; Li, C. J.; Chen, D. M.; Wang, C.; Wang, C. R.; Bai, C. L.; Wang, Y. G. *J. Mater. Chem.* **2004**, *14*, 914.
(16) Guo, Y. G.; Li, C. J.; Wan, L. J.; Chen, D. M.; Wang, C. R.; Bai, C. L.; Wang, Y. G. *Adv. Funct. Mater.* **2003**, *13*, 626.
(17) Li, C. J.; Guo, Y. G.; Li, B. S.; Wang, C. R.; Wan, L. J.; Bai, C. L. *Adv. Mater.* **2005**, *17*, 71.
(18) Kobayashi, K.; Tachibana, M.; Kojima, K. *J. Cryst. Growth* **2005**, *274*, 617.
(19) Minato, J.; Miyazawa, K.; Suga, T. *Sci. Technol. Adv. Mater.* **2005**, *6*, 272.
(20) Minato, J.; Miyazawa, K. *Carbon* **2005**, *43*, 2837.
(21) Miyazawa, K.; Kuwasaki, Y.; Hamamoto, K.; Nagata, S.; Obayashi, A.; Kuwabara, M. *Surf. Interface Anal.* **2003**, *35*, 117.
(22) Miyazawa, K.; Minato, J.; Yoshii, T.; Fujino, M.; Suga, T. *J. Mater. Res.* **2005**, *20*, 688.
(23) Wang, L.; Liu, B. B.; Liu, D.; Yao, M. G.; Hou, Y. Y.; Yu, S. D.; Cui, T.; Li, D. M.; Zou, G. T.; Iwasiewicz, A.; Sundqvist, B. *Adv. Mater.* **2006**, *18*, 1883.
(24) Jin, Y. Z.; Curry, R. J.; Sloan, J.; Hatton, R. A.; Chong, L. C.; Blanchard, N.; Stolojan, V.; Kroto, H. W.; Silva, S. R. P. *J. Mater. Chem.* **2006**, *16*, 3715.
(25) Hu, J. S.; Guo, Y. G.; Liang, H. P.; Wan, L. J.; Jiang, L. *J. Am. Chem. Soc.* **2005**, *127*, 17090.
(26) Rao, A. M.; Zhou, P.; Wang, K. A.; Hager, G. T.; Holden, J. M.; Wang, Y.; Lee, W. T.; Bi, X. X.; Eklund, P. C.; Cornett, D. S.; Duncan, M. A.; Amster, I. J. *Science* **1993**, *259*, 955.
(27) Kratschmer, W.; Lamb, L. D.; Fostiropoulos, K.; Huffman, D. R. *Nature* **1990**, *347*, 354.
(28) Davydov, V. A.; Kashevarova, L. S.; Rakhmanina, A. V.; Senyavin, V. M.; Ceolin, R.; Szwarc, H.; Allouchi, H.; Agafonov, V. *Phys. Rev. B* **2000**, *61*, 11936.
(29) Bethune, D. S.; Meijer, G.; Tang, W. C.; Rosen, H. J.; Golden, W. G.; Seki, H.; Brown, C. A.; Devries, M. S. *Chem. Phys. Lett.* **1991**, *179*, 181.
(30) Iwasa, Y.; Arima, T.; Fleming, R. M.; Siegrist, T.; Zhou, O.; Haddon, R. C.; Rothberg, L. J.; Lyons, K. B.; Carter, H. L.; Hebard, A. F.; Tycko, R.; Dabbagh, G.; Krajewski, J. J.; Thomas, G. A.; Yagi, T. *Science* **1994**, *264*, 1570.
(31) Ramm, M.; Luger, P.; Zobel, D.; Duczek, W.; Boeyens, J. C. A. *Cryst. Res. Technol.* **1996**, *31*, 43.
(32) Sun, Y. P.; Bunker, C. E. *Nature* **1993**, *365*, 398.
(33) Nath, S.; Pal, H.; Palit, D. K.; Sapre, A. V.; Mittal, J. P. *J. Phys. Chem. B* **1998**, *102*, 10158.
(34) Alargova, R. G.; Deguchi, S.; Tsujii, K. *J. Am. Chem. Soc.* **2001**, *123*, 10460.
(35) Bokare, A. D.; Patnaik, A. *J. Phys. Chem. B* **2005**, *109*, 87.
(36) Mayers, B.; Xia, Y. N. *Adv. Mater.* **2002**, *14*, 279.
(37) Krueger, G. C.; Miller, C. W. *J. Chem. Phys.* **1953**, *21*, 2018.
(38) Matijevic, E. *Langmuir* **1994**, *10*, 8.
(39) Aizenberg, J.; Black, A. J.; Whitesides, G. M. *Nature* **1999**, *398*, 495.
(40) Lucia, L. A.; Yui, T.; Sasai, R.; Takagi, S.; Takagi, K.; Yoshida, H.; Whitten, D. G.; Inoue, H. *J. Phys. Chem. B* **2003**, *107*, 3789.
(41) Balaban, T. S.; Leitich, J.; Holzwarth, A. R.; Schaffner, K. *J. Phys. Chem. B* **2000**, *104*, 1362.